THE MORPHOLOGY OF MAGNETIC PULSATIONS AT HALLEY BAY, 1974–76

By R. A. HAMILTON

ABSTRACT. The rubidium-vapour magnetometer (RVM) has been used at Halley Bay for the study of pulsations in the geomagnetic field with periods in the range 15–600 s. Two sensors measure variations in the NE and NW fields (from which variations in the conventional *H* and *D* fields can be computed) with a sensitivity of about 4 mm nT^{-1} and a third measures variations in the vertical field (*Z*) with a sensitivity of about 14 mm nT^{-1}.

Continuous pulsations (*Pc* 3) with a period in the range 15–45 s occur during the daytime, the frequency of occurrence being symmetrical about local geomagnetic noon; these are more frequent in winter than in summer. The period of *Pc* 3 is related to the magnetic activity; longer periods occur mainly during quiet magnetic conditions and shorter periods during disturbed conditions. A special form of *Pc* 3 with a period of about 15 s sometimes occurs at night.

Longer-period pulsations (*Pc* 4) with periods 45–150 s behave similarly to *Pc* 3. Pulsations (*Pc* 5) with periods 150–600 s occur mainly in the evening. Giant pulsations (*Pg*) occur mainly in the morning, are monochromatic with rather short periods in the range 50–100 s and are elliptically polarized in an E–W direction with a clockwise sense of rotation.

Irregular pulsations (*Pi* 2) occur mainly at night, with a maximum frequency around geomagnetic midnight, and are more frequent in winter than in summer. The period of the *Pi* 2 depends on the time of occurrence and on the magnetic activity; at any one time the period decreases to less than a half as the index of magnetic activity increases from 0 to 5, and for a constant magnetic activity the period decreases to about a half between 18.00 and 06.00 h local geomagnetic time. The polarization of *Pi* 2 is predominantly clockwise before and anti-clockwise after geomagnetic midnight.

The induced vertical field is small, amounting to about 0.1 of the horizontal field for periods of about 30 s to about 0.2 for periods around 200 s.

THE object of this paper is to present the facts on the variations of magnetic pulsations with other parameters as observed at Halley Bay, together with some notes on the data.

Geomagnetic observations have been made at Halley Bay (lat. 75° 31′S, long. 26° 40′W) since the beginning of the International Geophysical Year (IGY) in 1957. The British Antarctic Survey took over the station in 1959 from the Royal Society International Geophysical Year Antarctic Expedition which operated it during the IGY and the following year.

In the early years the only geomagnetic instruments were normal and storm sets of standard La Cour magnetographs, which can be used for studying pulsations with periods in the range 100–600 s. Between 1963 and 1968, the geophysicists operated a fluxgate magnetometer, which recorded variations in the three components of the geomagnetic field: *H* (S–N), *D* (W–E) and *Z* (vertical); the output was filtered so that the response was flat between 2 and 70 s period. An analysis of 3 months' recording by the fluxgate magnetometer was made by Finlayson (1967), and Westwood (1967) made a further study of pulsations during the four solsticial months, June and December 1963 and 1964. The data were used by Stuart and Macintosh (1970), Stuart (1972) and Sherwood and others (1973).

A rubidium-vapour magnetometer (RVM) (described below) was installed in 1971. At first measurements were made of *H* only but a three-component system was installed in 1972, though the *Z*-component sensor operated only fitfully until 1974. An initial study of 10 months' recording was made by Kaiser and others (1977), and Stuart (1975*a*, *b*, 1976) has compared features on the records with those recorded at St. Anthony, the conjugate station in the Northern Hemisphere. Magnetic tape recording was introduced in July 1976, thus enabling data to be read into a computer and providing a more powerful tool for making a detailed study of geomagnetic pulsations. The time is opportune, therefore, to review the results of the analysis of the chart recordings. This report presents the results of a study of the morphology of geomagnetic pulsations at Halley Bay in the period 1974–76.

THE RUBIDIUM-VAPOUR MAGNETOMETER

General principle

In a magnetic field the energy levels of the 794.6 nm D_1 line of rubidium are split, due to the

Zeeman effect, with sub-levels whose frequency separation is proportional to the field, and is equal to the precession frequency of the atoms. For ^{85}Rb this frequency is approximately $4.667B$ Hz when B is a field measured in nT; at the Earth's surface it is a radio frequency of the order of 100 kHz. If circularly polarized light is passed through rubidium vapour, it produces momentary alignment of the atomic dipoles in the direction of the light beam and, if this is inclined to the direction of the magnetic field, the atomic dipoles will precess about the field. The phases of the dipoles are randomly distributed but, if a small rotating magnetic field with a frequency equal to the precession frequency is imposed, resonance occurs and the dipoles will precess in phase. The absorption of the light by the dipoles varies with their orientation to the light beam and passes through a maximum and minimum in the course of one precession, and therefore the transmitted light is modulated at the precession frequency. If the light is focussed on a photocell, the modulated output can be amplified, phase-shifted and fed back to provide the rotating magnetic field. Thus a self-oscillating system is produced which resonates at the precession frequency, and the strength of the magnetic field can be determined from this frequency.

The sensing head

The light source is an electrodeless rubidium lamp maintained by a 100 MHz oscillator. Light from this lamp is filtered by an interference filter, which transmits only the D_1 line, and is circularly polarized by a polaroid filter. The light then passes through a gas cell about 20 mm long and 25 mm diameter containing rubidium vapour and a nitrogen buffer. A heating unit maintains the gas cell at a temperature of about 45°C. The transmitted light passes through a lens, which focuses it on a silicon photocell.

The magnetometer assembly

It is thus necessary to neutralize the vertical field (Z) when we wish to measure the horizontal field (H) or vice versa. Furthermore, the declination (D) cannot be measured directly. Consequently, two bias fields of magnitude $0.707H$ are set up at 45° relative to H, giving the skew components (S) in the NE and NW directions. H and D can then be derived.

The magnetometer assembly consists of two similar magnetometers for measuring the two skew fields and a third for measuring the vertical field.

A skew-field magnetometer comprises a sensor head and the two separate Helmholtz coils mounted on a turn-table. The coils and the turn-table are made of Tufnol. The large coil (Z coil), of 40 cm diameter and 75 Ω resistance, is used to annul the vertical component Z, while the smaller, S coil, of 20 cm diameter and 60 Ω resistance, is used to annul the skew component which is not being measured. Both coils have three levelling feet of non-magnetic brass and can be levelled relative to the turn-table. The turn-table has its own levelling feet and carries two small levels of sensitivity about 4×10^{-4} radians mm^{-1} (80″ mm^{-1}) and 1° graduations within 15° of the four 90° positions. The sensor is held at the centre of the small coil with its axis inclined at 45° to the vertical and to the derived skew field so as to ensure optimum signal-to-noise ratio.

The Z-field magnetometer is simpler, having only one coil (H coil) similar to the S coil.

At most observatories all the coils of a RVM are fitted with thermistors, potted on to the coil former, to compensate the coil current, and thus the biasing field, for temperature changes in the resistance of the coil. At Halley Bay, however, the RVM is housed in a tunnel below the snow surface, where temperature changes are very slow. Although continuous measurements were not made, it is most unlikely that there was ever a significant diurnal variation in temperature, the greatest change detected from one day to the next being $\frac{1}{2}$°C even when there were large changes of temperature at the surface.

The coil constants are about 2.3 μA nT^{-1}, so the coil current ranges from 0.04 A for the S coil to about 0.10 A for the Z coil.

The H field can be measured by the skew magnetometers by switching off the current in the S coils, and the total field (F) can be measured by all the magnetometers by switching off all the coil currents.

Measurement of the precession frequency

The frequency (L) of the radio-frequency signal is determined using the technique in which the number of oscillations of the stable reference frequency (f, 500 or 1 000 kHz) is counted for the period of a selected number of cycles of the precession frequency. The counting interval (t) is determined by the number of binary counters (b) in a period counting chain; b can be varied from 11 to 19.

If n is the count,

then $n = ft$,

where $t = 2^b L^{-1}$.

But $L = 4.667B$,

so $B = 0.2143 n^{-1} 2^b f$ nT.

Each sensor is sampled independently and the signals are taken to three independent frequency counters. The counting intervals are about 0.2 s for the S fields and about 1.3 s for the Z field, the counts being about 1.2×10^5 and 1.3×10^6, respectively.

The analogue record

The eight least significant binary digits of the count are converted to analogue forms so as to produce a full-scale deflection of 0 to 192 counts with scale jumps of 128 counts where the count goes below 0 or above 192.

A Rikadenki recorder is used with an Intek paper chart of 250 mm width. Thus, each of the three traces has a range of about 80 mm and a jump range of about 50 mm. The paper speed is normally 5 mm min^{-1}; at this speed the chart runs for 3 d. The station clock makes time marks on the chart at each minute with special marks at the hour. This clock is checked daily by radio signals and the error is normally less than $\pm$ 3 s.

Sensitivity of the magnetometers

The equation relating the count n to the field B is

$$n = 0.2143\ 2^b f B^{-1}.$$

So the sensitivity is given by

$$dn/dB = -0.2143\ 2^b f B^{-2}.$$

It is more useful to determine the scale value

$$dB/dn = 4.667\ B^2\ 2^{-b} f^{-1}.$$

For the skew fields ($S = 1.43 \times 10^4$ nT), values of $b = 14$ and $f = 5 \times 10^5$ have been found suitable giving

$dS/dn = 0.12$ nT per count and a range of 15 nT per jump of 128 counts.

On the chart, the range of a jump is about 50 mm, so the chart scale value is 0.3 nT mm^{-1}, with a full-scale deflection of 22.5 nT.

For the vertical field ($Z = 4.2 \times 10^4$ nT), values of $b = 18$ and $f = 10^6$ are used, giving

$dZ/dn = 0.03$ nT per count, a range at 4.0 nT per jump of 128 counts, so that the chart scale value is 0.08 nT mm^{-1}.

The high sensitivity is required as the amplitude of pulsations in the vertical field is generally small.

The sensitivity of the S field (RVM) is about 20 times that of the standard H field La Cour magnetometer, while for the Z field the ratio is about 90.

The effect of errors in levelling and in the biasing field

Measurement of skew field. Let the biasing Z field be $Z + dZ$ at a small angle α to the vertical and at an angle θ to the skew field (S) in the horizontal plane. The components of the field are:

$$(Z + dZ)\cos\alpha - Z = dZ - \tfrac{1}{2}\alpha^2 Z + \ldots$$
$$S + (Z + dZ)\cos\theta \sin\alpha = S + \alpha Z \cos\theta + \ldots$$
$$(Z + dZ)\sin\alpha \sin\theta = \alpha Z \sin\theta.$$

The measured field $S' = S + \triangle S$ is given by

$$S'^2 = S^2 + 2\alpha SZ \cos\theta + \alpha^2 Z^2 + \ldots \quad (1)$$

giving $\Delta S = \alpha Z (\cos\theta + \frac{1}{2}\alpha Z/S)$.

Thus, an error in the levelling of the neutralizing Z coils produces an error in S which is proportional to the tilt. At Halley Bay, which is situated on a moving ice shelf, it is difficult to keep scientific instruments level but α should not exceed 10^{-3} (an easily detectable bubble movement of 2.5 mm). Z is 4.2×10^4 nT and Z/S is 2.9. So the maximum error in S is likely to be about 40 nT. This is a slowly varying error and, for the study of magnetic pulsations, is of no consequence.

The effect in the S field of fluctuations in the Z field of amplitude dZ, due to natural pulsations or fluctuations in the neutralizing Z field, is obtained by differentiating Equation (1) giving

$$2S'dS'/dZ = 2\alpha S \cos\theta + 2\alpha^2 Z$$

or, writing S for S'

$$dS/dZ = \alpha \cos\theta + \ldots .$$

Thus the maximum value of dS/dZ is α, i.e. around 10^{-3} or less. Pulsations in the Z field will have no effect on the S field and fluctuations in the biasing field of 1% will produce fluctuations in the S field of only 0.4 nT; in practice the stability of the current is better than 10^{-3}.

Measurement of the vertical field, Z. The equation corresponding to (1), relating the measured vertical field Z' when the biasing field is inclined at a small angle α to the horizontal, is

$$Z'^2 = Z^2 + 2\alpha HZ + \alpha^2 H^2 + \ldots, \quad (2)$$

whence $\Delta Z + \alpha H$ and $dZ/dH = \alpha$.

Again, αH is a slowly changing error of no consequence and the effect of fluctuations in the biasing H field on the Z field is smaller than in the previous case. The value of α is two orders of magnitude less than induction coefficients between natural pulsations in the H and Z fields.

The very small errors in the measured field arising from errors in the biasing fields is one of the virtues of the RVM. At most stations, where the magnetometers stand on a rigid base, the angle α can be made smaller than at Halley Bay, resulting in even smaller errors due to fluctuations in the biasing fields.

Orientation effects

Usher and others (1964), using an early model of an RVM, found that the maximum signal occurred where the light beam was inclined at 45° to the magnetic field and that self-oscillation occurred within ± 35° of this optimum position.

Because of the complex line structure of the rubidium, the frequency of precession depends on the inclination of the light beam relative to the magnetic field. The error of a field measurement due to orientation may amount to about 5 nT over the whole angular range within which self-oscillation occurs. Thus, the RVM is not strictly an absolute instrument. However, for a fixed orientation no drift occurs and relative measurements can be made with high precision.

Magnetic tape recording

In 1976, a modified version of the RVM was installed which records on magnetic tape in

addition to the paper chart. In this version, sampling of the three sensors is initiated simultaneously by a clock, which controls the function of the digital recording system. The period of the sampling cycle is 2.5 s. The chart record is less smooth than previously but more accurate analysis of the digital record on the magnetic tape can be carried out on a computer. Continuous recording on magnetic tape commenced in July 1976.

The RVM assembly in use at Halley Bay was designed and built by the staff at the Geomagnetism Unit of the Institute of Geological Sciences, Edinburgh.

Calibration of the Magnetometer

Precession frequency measurements

The following measurements are made at the time of changing the chart (at 3 d intervals), provided the trace at the time is fairly undisturbed:

i. The three precession frequencies f(NE), f(NW) and f(Z) are measured.
ii. The current in the two S coils is switched off and measurements of f(H) are made on the two skew magnetometers.
iii. The currents in the H coil and the two Z coils are switched off and measurements of f(F) are made on all three magnetometers.

The three values of f(F) are compared; they may differ slightly due to sensor or site-difference errors. The range normally found is about 200 in 220 000, i.e. 1 in 10^3.

The two values of f(H) are now compared. These have differed by as much as 500 Hz in 100 000, i.e. 5 in 10^3; the difference is due to errors in the biasing fields or in levelling.

The value of $[f^2(H) + f^2(Z)]^{\frac{1}{2}}$ is compared with f(F); the values normally differ by less than 1 in 10^3.

The values of f(NE) and f(NW) normally differ by less than 0.5% and their mean does not exceed 0.707 f(H) by more than 0.25%. Calibrations are not made when interesting features are present or when the chart needs changing.

Comparison with standard La Cour magnetographs

The scale value and the sense of measurement are occasionally checked by comparing the RVM record with that of the standard La Cour magnetograph, which is itself checked by absolute measurements. For the vertical field the comparison is easy; one chooses a good bay on the La Cour trace, counts the number of jumps in the RVM chart over the same period and then compares the two measurements of the change in Z.

The comparison of the horizontal fields is not so easy as the La Cour measures changes in the N and E fields, and the RVM changes in the NE and NW fields, and these rarely reach slowly moving values simultaneously. However, there are occasions when fairly large movements can be measured with sufficient accuracy on the four traces, and Table I shows the result of comparisons made on several days in October 1974. In Table I, ΔNE and ΔNW are the skew-field changes (in nT), from which the conventional orthogonal field changes $\Delta H = (\Delta NE + \Delta NW)/2^{\frac{1}{2}}$

Table I. Comparison of changes in the horizontal geomagnetic field as measured by the La Cour (LC) and rubidium-vapour (RVM) magnetometers (unit nT)

Date	UT	ΔNE	ΔNW	ΔH		ΔE	
				RVM	LC	RVM	LC
1 October	05.35–06.00	15	−59	−31	−30	−52	−51
3 October	05.55–06.05	15	−34	−13	−17	35	35
4 October	02.25–02.50	36	−36	0	0	51	48
4 October	22.00–22.39	−159	57	−72	−76	−153	−150
5 October	21.00–21.20	−6	45	28	22	−36	−34

and $\Delta E = \Delta NE - \Delta NW)/2^{\frac{1}{2}}$ are calculated and compared with the values ΔH and ΛE measured by the La Cour magnetograph.

This test is important, not only to check on the scale value but to check the directions of movement, as an inadvertent reversal of leads is possible at several points in the system and would cause a change in the apparent sense of the perturbations which would not be self-evident. It is of especial importance to check on the movement of Z, for the magnetometer is designed for use in the Northern Hemisphere, where Z is conventially measured positive downwards, while in the Southern Hemisphere it is measured positive upwards.

Notes on the Observing Site

The geographical coordinates of the observatory at Halley Bay are:

lat. 75° 31′S, long. 26° 50′W.

The geomagnetic coordinates are:

lat. −65.6°, long. 24.1° (centred geomagnetic);
lat. −62.4°, long. 167.7° (eccentric geomagnetic).

The L value for a point 150 km above the observatory, based on IGRF (1975), is 4.4.
The $K = 9$ lower limit is 1 500 nT.
Approximate values of the geomagnetic field are:

$H = 20\,000$ nT,
$D = 359°$,
$Z = 42\,000$ nT,
$F = 47\,000$ nT.

The observatory is near sea-level on the ice shelf about 2 km from the ice edge. The ice shelf is moving and the quoted position is that in 1977; the latitude is almost constant but west longitude increases by about 1′ year^{-1}. The ice shelf rotates slowly so the azimuth of the magnetic meridian is continually changing.

The RVM is housed below the snow surface in a T-shaped tunnel complex which was constructed in 1973; each arm is 20 m long, 2.2 m high and 1.4 m wide. In January 1974, the roof of the tunnel was covered by approximately 30 cm of snow and this had increased to 3 m by December 1976, giving good thermal insulation. During 1974 the temperature in the tunnel ranged from about −10°C in summer to about −25°C in winter, but then it became effectively constant at approximately −11°C.

From 1974 to 1976, the NE and NW sensors were placed near the ends of the east and west arms of the tunnel, so they were nearly 40 m apart. The Z sensor was placed about 12 m from the eastern end of the tunnel (Fig. 1). The control unit was housed in a small heated room built just to the west of the centre of the tunnel. The sensors were mounted on lengths of telepho[illegible] pole sunk into the consolidated snow beneath the tunnel floor.

The LMT of geomagnetic midnight is about 01.24 UT; this is the mean of the values obtained by Sherwood and others (1973), who used five methods of calculation.

The data considered in this paper are confined to the interval 22 February 1974, when recording resumed after the construction of the tunnel, to 30 December 1976, the last record to be sent out by the relief ship early in 1977. Thus the interval does not strictly cover the 3 year period 1974–76 and, when statistically necessary, a correction has been made in the analysis of the records for the missing 53 d.

Geomagnetic Pulsations

Definitions

Geomagnetic pulsations may in general be divided into two classes: those of a regular and mainly continuous character and those with an irregular pattern or wave form. Continuous

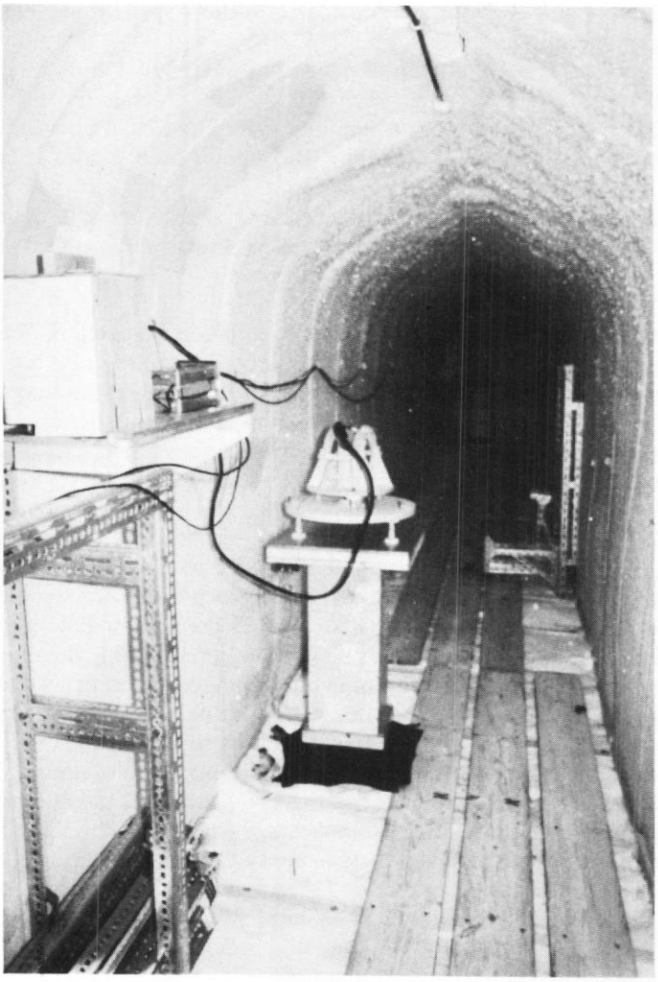

Fig. 1. View in the snow tunnel looking east. The Z sensor is in the foreground and the NE sensor is at the end of the tunnel.

Pulsations (*Pc*) generally last for several hours and are subdivided into groups depending on their period as follows:

Notation	*Period range* (s)
Pc 1	2–5
Pc 2	5–10
Pc 3	10–45
Pc 4	45–150
Pc 5	150–600

Irregular pulsations (*Pi*) are divided into two groups as follows:

Notation	*Period range* (s)
Pi 1	1–40
Pi 2	40–150

The groups *Pi* 1, *Pc* 1 and *Pc* 2 are not considered in this paper as they cannot be adequately identified at the paper speed used.

The IAGA definition of *Pi* 2 is "a train of pulsations of irregular shape and beginning mostly impulsively, with period 40–150 seconds consisting of several series of oscillations each lasting about 10 minutes (*Pi* 2 corresponds to the previous *Pt*)". The *Pi* 2 oscillations are well damped, they often precede or accompany a bay, and the whole phenomenon does not often last for more than an hour.

In addition, there is a third class, giant pulsations (*Pg*), which is defined by IAGA as "exceptional pulsations of very great period and regularity, with sufficient relative amplitude".

Analysis of the records

These definitions of the classes of pulsations are imprecise and allow much latitude in the subjective analysis of the records. The quality of the records, in particular the background noise, also affects the analysis—clearly it is much easier to detect pulsations in magnetically quiet than in magnetically disturbed conditions. Special tests show that two experienced analysts pick out the same events, provided they are fairly good, and it is only in the selection of doubtful events that opinions differ. Furthermore, when a record is re-analysed after a period of a year or mo the second analysis is substantially the same as the first. This gives some confidence in the analysis which must, from the nature of the events, be subjective and somewhat imprecise.

The procedure has been to run through each chart and to enter in a notebook the details of each event—the type (*Pi, Pc* or *Pg*), the date and time of beginning and ending, the predominant period and a quality marking in the range: poor, rather poor, fair, quite good, good and very good. Fair is used in most cases. This denotes an event of a reasonably definite period, the reality of which is not in serious doubt. A good event is one which clearly satisfies the definitions and is of good quality, with a definite period. An event would be classed as poor, if the trace was difficult to analyse and there was therefore doubt about its reality or the ability to measure it in a meaningful way, or, if the event showed a very variable period. No attempt has been made to measure the amplitude at the analysis stage, as this is so variable, though notes such as "small amplitude but clear" or "large amplitude" are sometimes entered.

Pc are rarely really continuous; usually they disappear and re-appear intermittently. When the pulsations clearly cease for an hour or more and then begin again, the two parts are listed as two separate events. The period of *Pc* fluctuates and a tolerance of ± 5 s is accepted, e.g. a *Pc* in which the period varied between 30 and 40 s would be listed as having a period of 35 s but, if the period increased to 45 s, it would be listed as a new *Pc*.

Fig. 2 is an example of *Pc* 3; it shows three intervals of 18 min of the NW trace at approximately 3 h intervals on 17 March 1975. The background is slightly disturbed but the pulsations are clear and show a gradual increase of period from 40 s in the first section to 50 s i the second, and to 60 s in the third section.

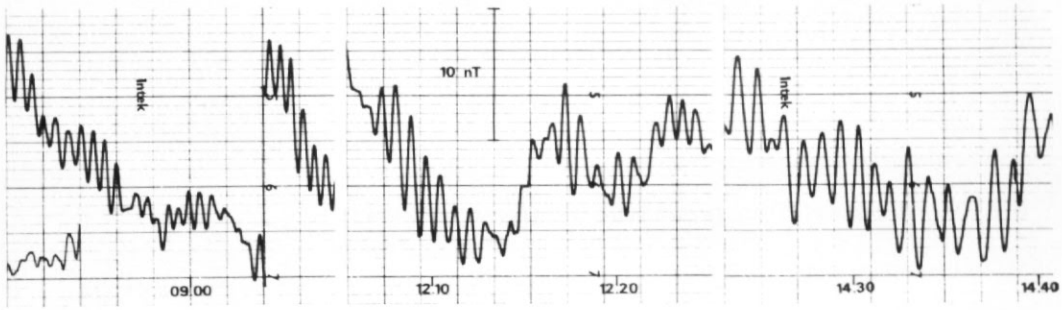

Fig. 2. Three sections of the NW trace on 17 March 1975; *Pc* 3 with slowly increasing period.

Fig. 3 is an example of a typical *Pc* 3 of 30 s period; it shows well the characteristic constancy of period, with typical variations of amplitude. This *Pc* 3 lasted from 13.00 to 18.15 on 14 September 1975.

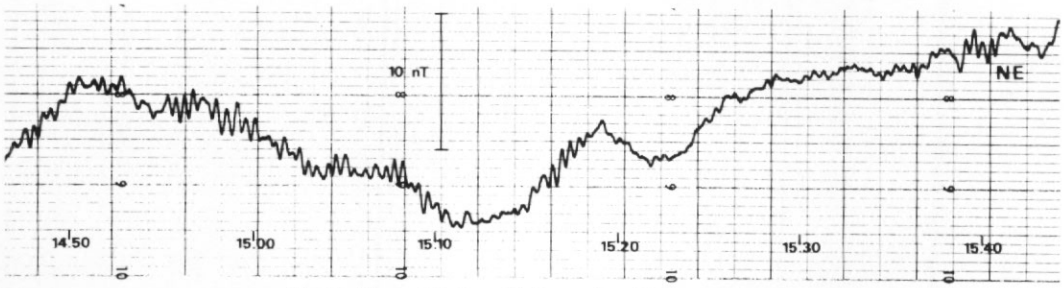

Fig. 3. Typical *Pc* 3 on 14 September 1975; period 30 s.

Pi are more difficult to identify, as by definition they are irregular. However, though irregular in amplitude, most have fairly well-defined periods. The train may consist of only two series of pulsations and single series of pulsations occur quite often. On some occasions the train continues for a few hours. They mainly occur before or during bays. Sometimes the pulsations occur before the onset of a bay and then cannot be detected while the field is changing very rapidly, reappearing at the peak of the bay where the field movement is slow.

Fig. 4 is a good example of a *Pi* 2 of period about 130 s which occurred on 7 December 1974; it shows clearly the impulsive beginning and the damping. The subsequent series of oscillations in the train, which lasted for 70 min, is not shown.

The cases of *Pg* found have been characterized by their very great regularity, though they have not been of very great period. They are striking in appearance, as illustrated in Fig. 5, which shows a packet of waves of period 57 s that occurred on 12 June 1975 and lasted about 20 min.

Spectral analysis of geomagnetic pulsations

Sections of traces which show geomagnetic pulsations have been digitized to enable a spectral analysis of the sample to be made. The digitizer measures x and y coordinates to an accuracy of 0.01 cm.

For *Pc* 3, sections of about 20 min duration are normally selected and the coordinates of about 200 points measured, including those at the top and bottom of each jump. The measurements are fed into the computer which removes the jumps and then interpolates coordinates equispaced at 5 s intervals. The scale values of the three components are then fed in and the skew components are rotated, giving a set of values of the variation of H, D and Z field about a mean value at 5 s intervals. The computer then carries out a Fast Fourier Transform (FFT) of those values. A typical result is given in Table II, which is the spectral analysis of the H and D components of the record of 17 March 1975 around 09.00 UT, the NW part of which is illustrated in Fig. 2. The second and third columns give the power, in units of $(\mathrm{nT})^2\mathrm{Hz}^{-1}$, of the H and D components of pulsations in the frequency band corresponding to the period in the first column. The fourth column gives the phase differences between the components, (—) implying clockwise rotation. The coherence (c), in the fifth column, is a measure of the correlation between the two traces at the given period. The computer then calculates the polarization characteristics and prints out the angle of polarization (φ) and the ellipticity (e, the ratio of the minor to major axis of the ellipse). In the full computer output, the values are given to three decimal points and, in addition, the cross-amplitude and the degree of polarization are given; these have been omitted from Table II, as have the data for periods longer than 90 s and shorter than 11 s.

For *Pc* 4, a longer section of record is analysed and an equispaced time interval of 12 s is chosen, while for *Pc* 5 the equispaced time interval is 30 s.

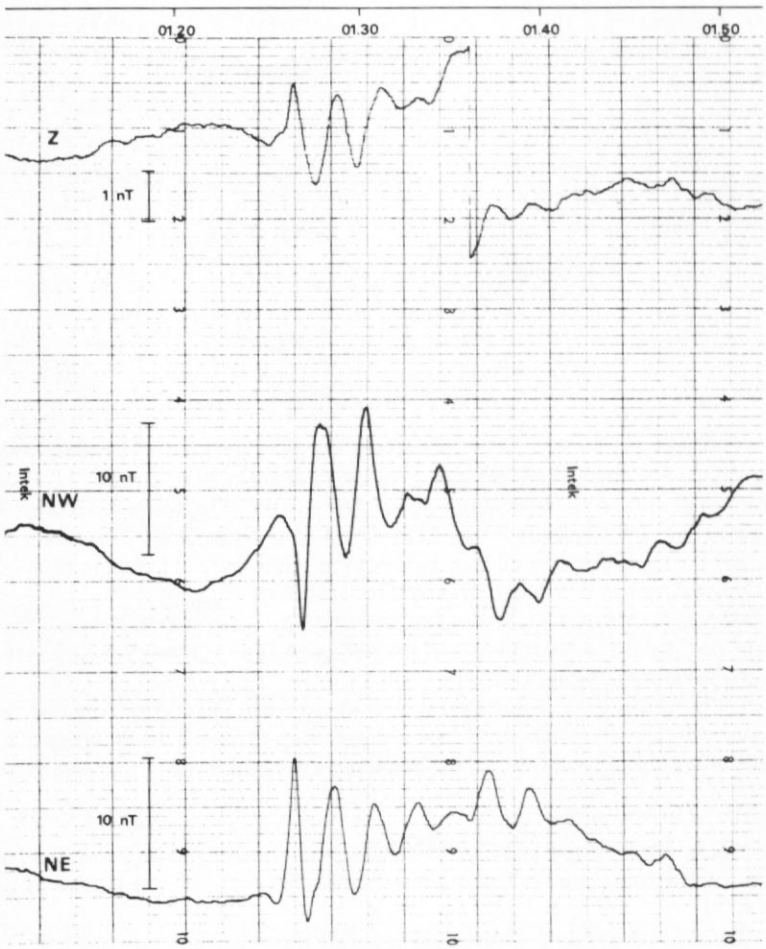

Fig. 4. *Pi* 2 on 7 December 1974; period 130 s.

The FFT programme allows only two components to be analysed at one time; the skew components are used to obtain power spectra and polarization characteristics of the *H* and *D* traces. When relations with the *Z* component are required, it is compared with one of the horizontal components.

Continuous Pulsations *Pc* 3

Analysis procedure

A preliminary analysis of *Pc* 3 events showed no appreciable change in their characteristics between vernal and autumnal equinox nor between short- and long-duration events. Accordingly, for the statistical analysis, the year has been divided into three seasons: summer: 22 October to 20 February; equinox: 21 February to 21 April and 22 August to 21 October; and winter: 22 April to 21 August—and only *Pc* events of 6 h duration or more have been considered.

Relation between Pc 3 and magnetic activity

Any study of pulsations must take into account the relation between frequency of occurrence and period of pulsations with magnetic activity.

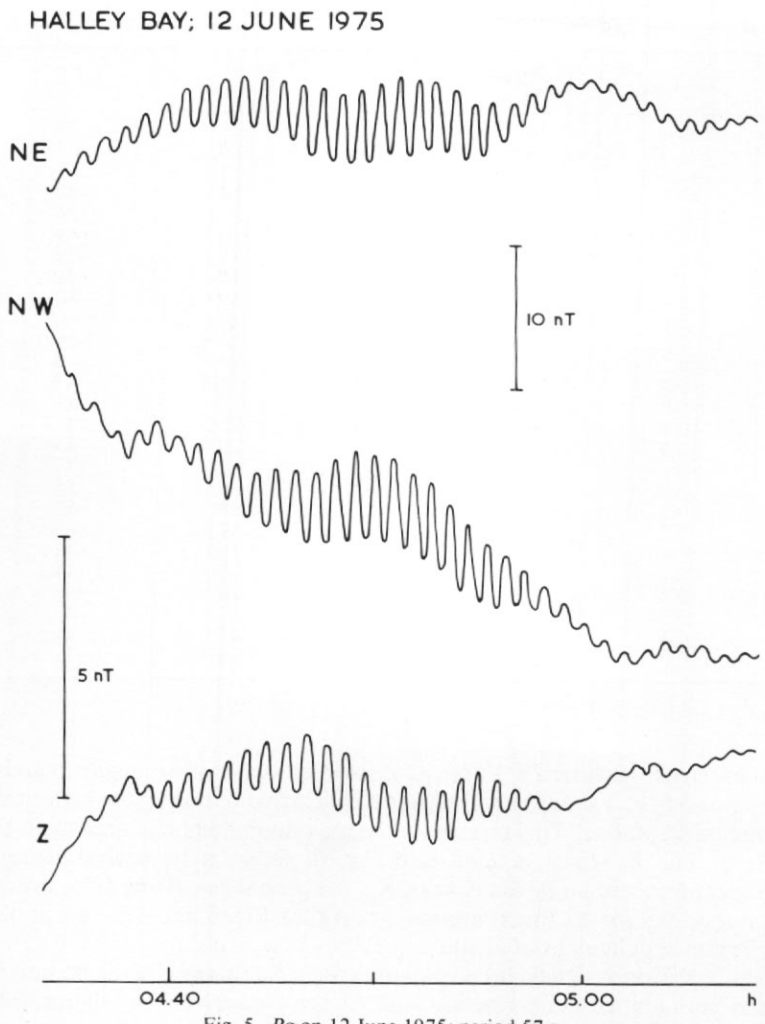

Fig. 5. *Pg* on 12 June 1975; period 57 s.

As *Pc* 3 activity occurs mainly in the period 04–18 UT, the analysis has been confined to this interval. First, the *Pc* 3 activity has been related to the K_p index at the time of the event. Selecting K_p 3 h intervals during which *Pc* 3 occurred for at least 2 h, the K_p index and the period t s of the event was noted; this gave 575 pairs of simultaneous values of K_p and t. The frequency of occurrence of *Pc* 3 events for each K_p value is given in Fig. 6. The *Pc* 3 events studied also exhibit the following features:

i. A decrease in number of events from 1974 to 1976 in sympathy with the change in 12 monthly mean sunspot numbers, 34.5, 16.0, 12.2, respectively.
ii. The frequency was greater in winter than in the other seasons.

In 1976 there was relatively little *Pc* 3 activity after the autumnal (March) equinox. This was, however, sunspot minimum.

The mean values of the period t of the *Pc* 3 events are given in Fig. 7. The dominant feature is a monotonic decrease in t from about 36 s at low activity to about 24 s when $K_p = 5$. No significant year-to-year or seasonal change is present.

TABLE II. FAST FOURIER ESTIMATE OF SKEW COMPONENTS OF TRACE 08.50–09.08, 17 MARCH 1975

Period (s)	*Power* *H*	*D*	*Phase*	*c*	φ	*e*
89.8	3.0	4.5	163	0.38	−59	0.13
70.1	4.3	6.5	−170	0.53	−56	0.07
57.5	12.0	17.5	−76	0.70	69	0.70
48.8	20.1	16.2	−160	0.66	−40	0.17
42.3	60.6	33.6	174	0.75	−34	0.05
37.4	114.9	77.0	−172	0.93	−39	0.07
33.5	63.5	29.0	176	0.97	−34	0.03
30.3	1.2	1.7	165	0.74	−51	0.13
27.7	0.4	0.4	−104	0.09	−80	0.49
25.5	0.3	0.2	−49	0.43	20	0.35
23.6	0.5	0.6	164	0.49	−54	0.13
22.0	0.2	0.7	−58	0.94	70	0.43
20.6	0.3	0.3	−137	0.50	−47	0.39
19.3	0.9	0.8	163	0.94	−43	0.15
18.2	0.9	0.9	179	0.95	−45	0.01
17.2	0.5	0.5	−179	0.93	−43	0.01
16.4	0.1	0.1	163	0.48	−47	0.15
15.6	0.2	0.4	167	0.83	−55	0.11
14.8	0.2	0.3	−171	0.96	−47	0.08
14.2	0.2	0.2	−165	0.93	−43	0.12
13.6	0.4	0.4	172	0.94	−44	0.07
13.0	0.4	0.4	175	0.90	−44	0.04
12.5	0.4	0.3	−170	0.93	−40	0.08
12.0	0.2	0.2	173	0.74	−37	0.05
11.6	0.2	0.1	−172	0.74	−36	0.07
11.2	0.2	0.2	−163	0.69	−51	0.14

c Coherence. φ Angle of polarization (in degrees). *e* Ellipticity.

In order to ascertain whether *Pc* 3 activity correlated better with magnetic activity before the *Pc* 3 event than during it, a similar analysis has been carried out using the highest value K_p (max) of K_p in the period 00–09 UT. This represents the maximum magnetic activity in the 9 h interval before the *Pc* 3. Fig. 8, which is similar to Fig. 6, shows a somewhat greater variation of probability of occurrence than in the case of K_p, the probability rising from around 0.1 for low K_p (max) to around 0.3 for K_p (max) around 3+. As for Fig. 6, the decrease at higher K_p (max) values could be due to difficulties of identifying *Pc* 3.

As with Fig. 7, the only significant variation is with K_p (max). This is summarized in Fig. 9. The changes in both amplitude and period with K_p are greater for the relation with K_p (max) in the earlier period than for the direct comparison.

A study of the cases where there was a marked change of K_p during the period 00–18 UT and of the anomalous cases where the K_p index was high and the period of the *Pc* 3 was 40 or 4[illegible] gave no hint of the existence of a better magnetic index. As it is easier to derive, and marginally better in the case of frequency of occurrence, the K_p (max) relationship has been adopted.

Table III gives the percentage frequency of occurrence of *Pc* 3 events of different periods for various values of K_p (max). This shows clearly the frequent occurrence of long-period *Pc* 3 with low K_p (max) and of the short-period *Pc* 3 with high K_p (max), and vice versa.

Recurrence of Pc 3

When analysing the records, one is aware of intervals of 6 d or more when *Pc* 3 does not occur at all or occurs only fitfully and is of poor quality. The middle dates of intervals of non-occurrence of *Pc* 3 are given in Table IV which is mainly derived from the original list of *Pc* 3.

Table IV also gives the days in the solar rotation interval corresponding to the central date of intervals of low *Pc* 3 activity. The tendency for the low-activity intervals to recur at the same time of the solar rotation interval is quite well marked.

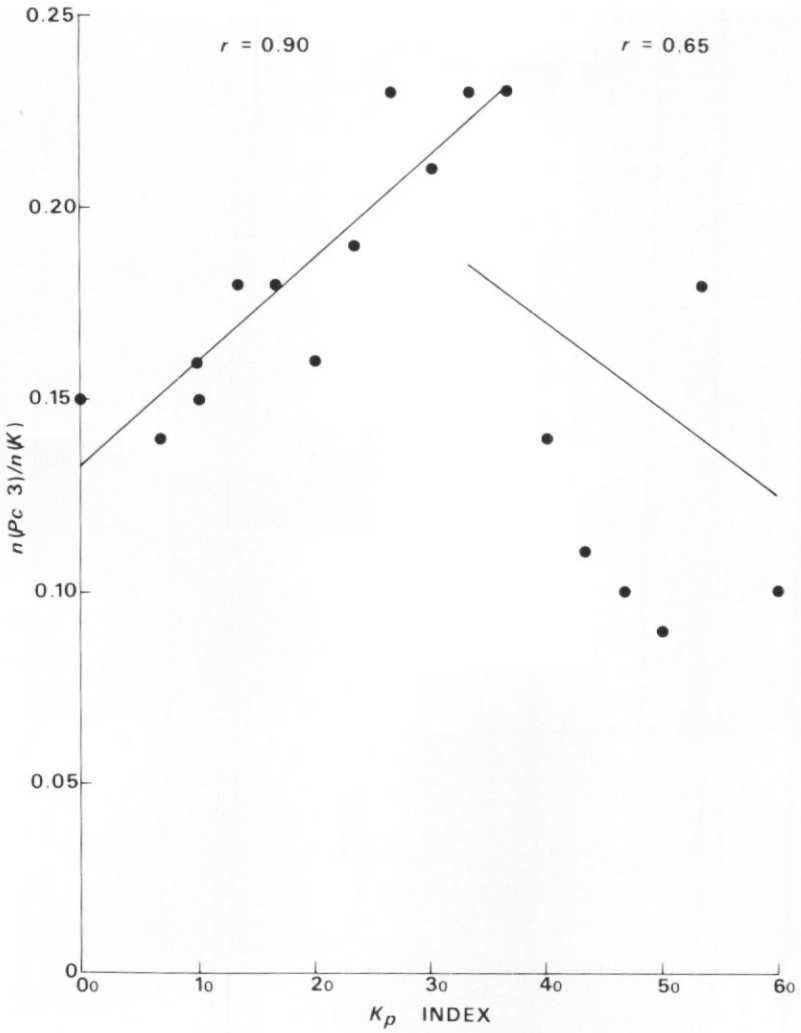

Fig. 6. Probability of occurrence of *Pc* 3 as a function of K_p index, showing regression lines and the correlation coefficients, *r*.

Night-time Pc 3

Fig. 10 is an example of a rare type of *Pc* 3 which was clearly visible on all components from 00.10 on 24 March to 12.00 on 25 March 1975; the period was 15 s and the maximum amplitude was 0.3 nT on the skew components, and 0.2 nT on *Z* (not shown). This type of *Pc* 3 is first seen near midnight with a period of 15–20 s and may persist throughout the day. It appears mainly during quiet magnetic conditions but can occur during moderate activity. This is clearly a special type of *Pc* 3 and has not been included in the statistical analysis.

Diurnal variation of Pc 3

The diurnal variation of *Pc* 3 is illustrated by Fig. 11 which gives the number of occasions when *Pc* 3 occurred in each hour. In all seasons there is a rather flat maximum in the middle of

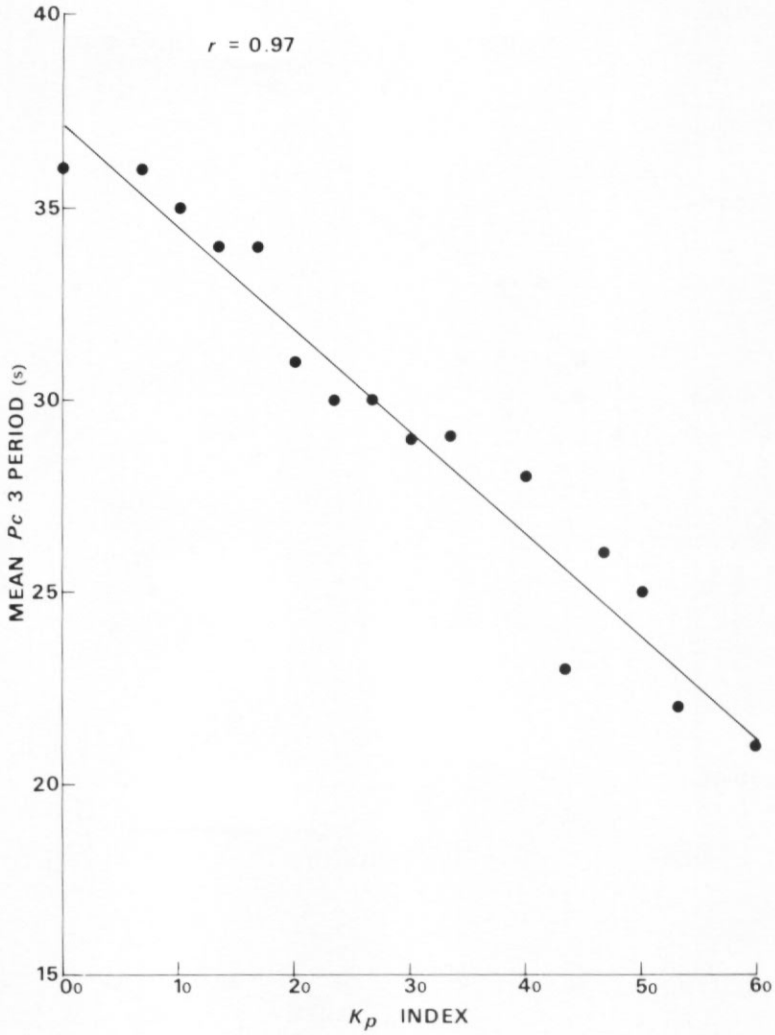

Fig. 7. Dependence of mean period of *Pc* 3 on K_p index; the regression line and correlation coefficient, *r*, are also shown.

the day. The median time for the whole period is 13.30 UT, which is very close to geomagnetic noon. The median times for each season differ little from this value.

There is a strong tendency for each *Pc* 3 event to be symmetrical about 13.30 UT. The mid-time of every event has been evaluated and Table V gives the frequency of occurrence of the various mid-times to the nearest half hour. The mean time is 13.26 UT and is substantially the same whatever the period of the pulsations.

Duration of Pc 3

The frequency of occurrence of *Pc* 3 events exceeding 6 h is given in Table VI; the mean duration is 9.3 h. The mean duration for *Pc* 3 of different periods was substantially the same, though those for periods 40 and 45 s were slightly less.

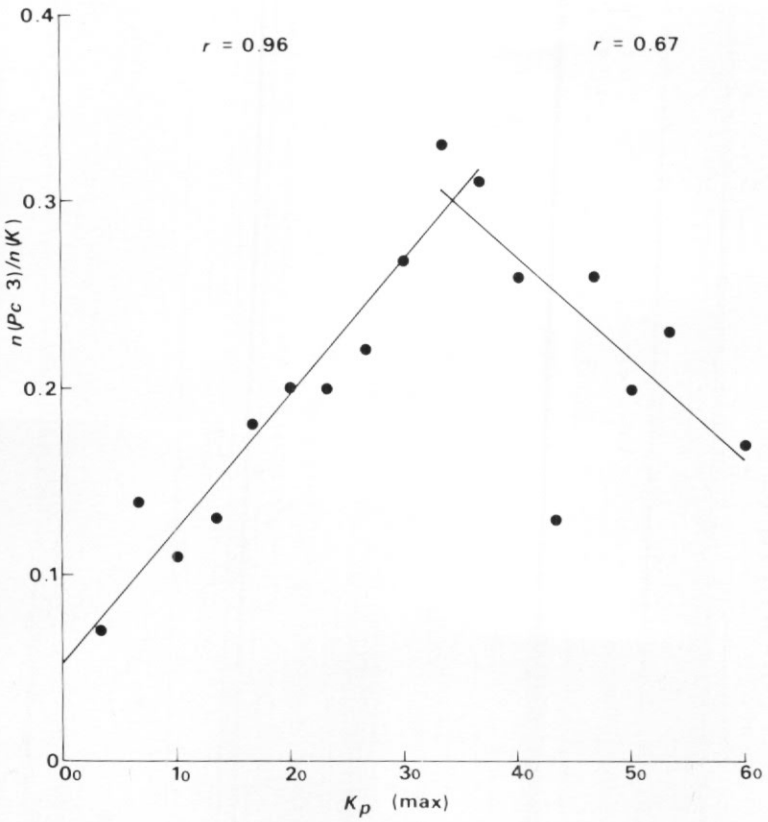

Fig. 8. Probability of occurrence of *Pc* 3 as a function of the highest value of K_p in the period 00–09 UT (K_p (max)). The regression lines and the correlation coefficients, *r*, are also shown.

Polarization of Pc 3

No analysis of the polarization of *Pc* 3 has been made. To make even a rough determination of the polarization requires measurements of the phase differences between the two skew components of better than one-quarter of a cycle, for a 30 s *Pc* corresponding to 0.6 mm, which approximates to the uncertainty in the correction for the parallax of the pens.

A detailed study of the polarization will be carried out when the tape recording with field-strength readings made every $2\frac{1}{2}$ s has been carried out for 1 year.

Continuous Pulsations: *Pc* 4, *Pc* 5 and *Pg*

Relation between Pc 4 and magnetic activity

The analysis has been carried out in the same way as in the case of *Pc* 3. The relation between *Pc* 4 events and the magnetic activity at the time of occurrence and in the previous 12 h was studied and the results are shown in Table VII. Table VIIa gives the percentage distributions of *Pc* 4 (and *Pc* 5) as functions of the value of K_p at the time of occurrence. Table VIIb gives the corresponding distribution as a function of the highest value of K_p in the 12 h period before the event. For comparison, Table VIIa also gives the percentage frequency of occurrence of the

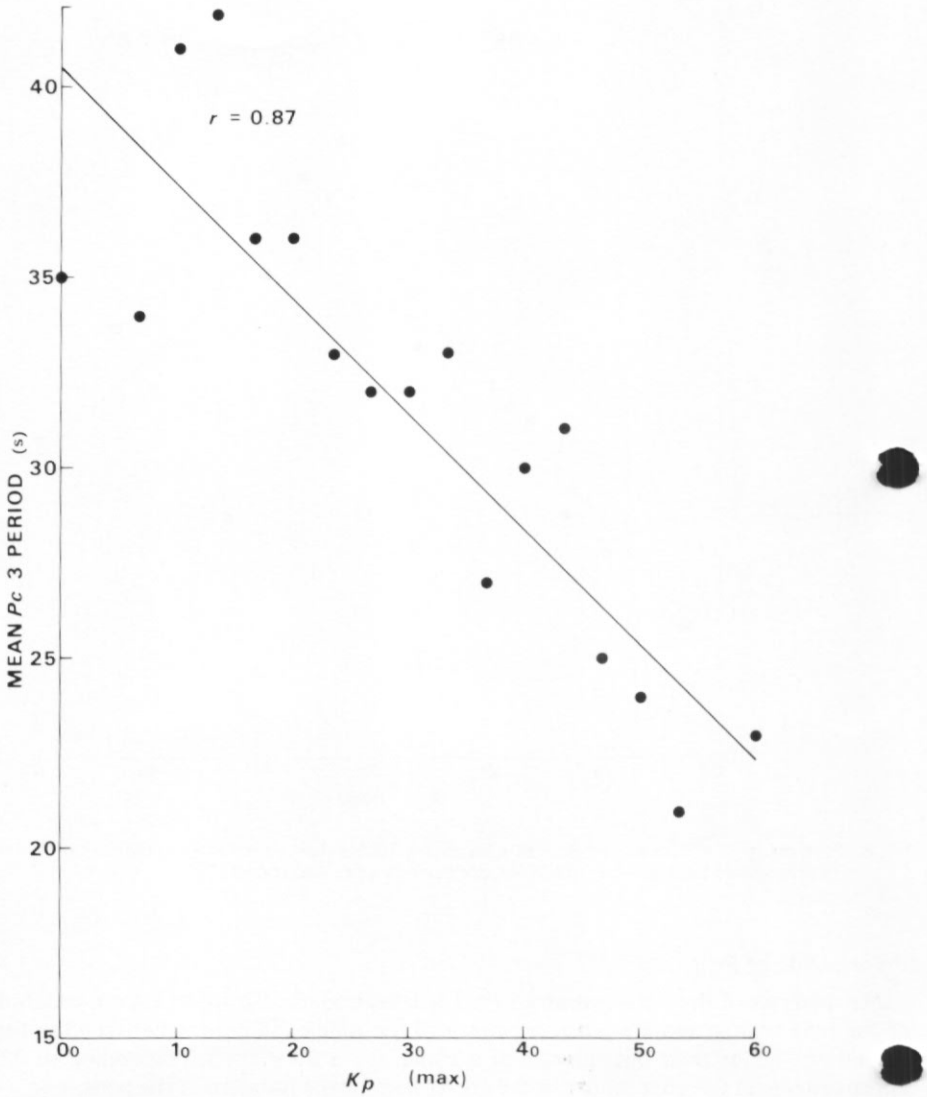

Fig. 9. Dependence of mean period of *Pc* 3 on the highest value of the K_p index in the period 00–09 UT (K_p (max)). The regression line and the correlation coefficient, *r*, are also shown.

TABLE III. PERCENTAGE FREQUENCY OF OCCURRENCE OF *Pc* 3 WITH PERIODS IN THE RANGE GIVEN IN COLUMN 1 FOR THE STATED K_p (max) VALUES

K_p (*max*)	1, 2	3	4	5, 6
Period (s)				
15, 20	2	13	16	44
25	5	5	24	30
30	24	29	24	19
35	22	23	16	5
40, 45	47	30	20	2

TABLE IV. CENTRAL DATE OF INTERVALS OF LOW *Pc* 3 ACTIVITY WITH DAY IN THE SOLAR ROTATION INTERVAL, *S*

1974		*1975*		*1976*	
Date	*S*	*Date*	*S*	*Date*	*S*
3 April	26	25 March	4	9 January	24
13 May	12	10 April	20	6 February	25
10 June	13	8 July	1	1 April	26
7 July	13	13 August	10	6 May	7
17 August	27	7 September	8	19 May	20
16 September	2	5 October	9	13 July	21
18 October	6	2 November	10	13 August	24
13 November	7	30 November	11	10 September	25
		25 December	9	5 October	23
				3 November	25
				1 December	26

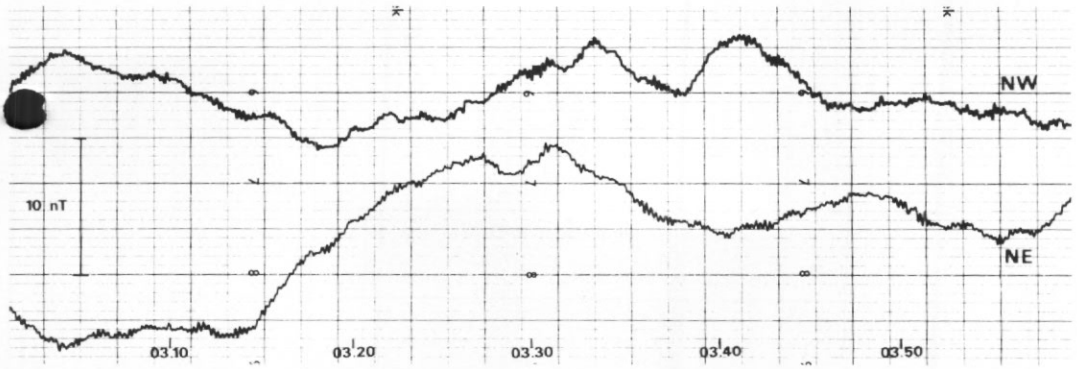

Fig. 10. Night-time *Pc* 3 on 24 March 1975; period 15 s.

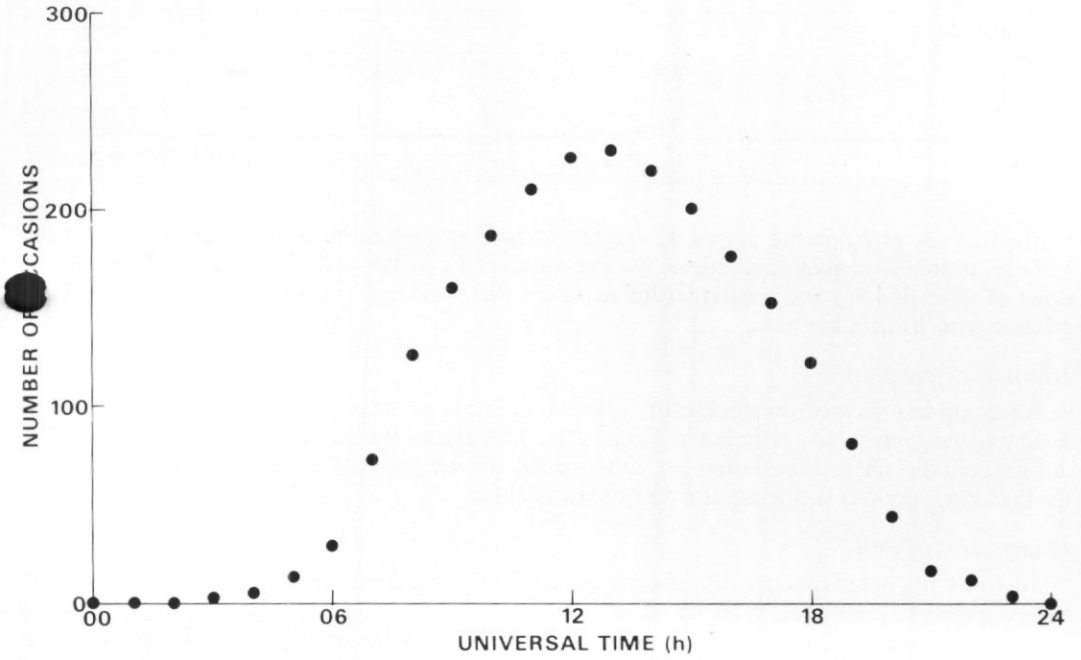

Fig. 11. Diurnal variation of *Pc* 3 occurrence observed from 1974 to 1976.

TABLE V. FREQUENCY OF OCCURRENCE OF *Pc* 3 EVENTS WHOSE MID TIME OF OCCURRENCE IS GIVEN IN ROW 1

Mid time (UT)	$9\frac{1}{2}$ or less	10	$10\frac{1}{2}$	11	$11\frac{1}{2}$	12	$12\frac{1}{2}$	13	$13\frac{1}{2}$	14	$14\frac{1}{2}$	15	$15\frac{1}{2}$	16	$16\frac{1}{2}$	17	$17\frac{1}{2}$ or more
Number of events	7	8	6	20	6	20	25	23	18	30	17	14	15	12	8	6	8

TABLE VI. FREQUENCY OF OCCURRENCE OF *Pc* 3 EVENTS OF DURATION GIVEN IN COLUMN 1

Duration (h)	*Number of events*	*Cumulative %*
6	48	20
7	32	33
8	34	47
9	30	59
10	25	70
11	19	77
12	23	81
13	11	91
14	6	94
15	9	98
16	3	99
17	3	100

Mean duration 9.3 h.

TABLE VII. CORRELATION BETWEEN *Pc* 4 AND *Pc* 5 WITH MAGNETIC ACTIVITY

(a)	K_p	0, 1	2	3	4	5	> 5
	Pc 4	27	23	32	13	4	
	Pc 5	38	22	21	16	3	
	K_p (15–18)	29	25	23	15	6	2
(b)	K_p (12 h)	0, 1	2	3	4	5	> 5
	Pc 4	12	25	24	23	14	2
	Pc 5	19	26	25	12	15	3
	K_p (03–15)	10	23	28	21	13	5

The figures in the table give the percentage frequency of occurrence of *Pc* 4 and *Pc* 5 for the values of K_p given at the top of each column, and the frequency of occurrence of the K_p value (see text).

various values of K_p in the period 15–18 UT (at time of maximum occurrence of *Pc* 4). Table VIIb gives the percentage occurrence for the value of K_p in the period 03–15 UT. The distributions of *Pc* 4 and K_p are indistinguishable within the sampling error, showing that there is no relation with K_p in either case.

Diurnal variation of Pc 4

An initial test showed no significant seasonal variation in the diurnal variation of *Pc* 4 and all available data have been included in Table VIII. This shows the number of occurrences of *Pc* 4 in four period groups. The diurnal variation for the shorter-period *Pc* 4 is similar to that of *Pc* 3; for the longer periods the maximum tends to occur later.

Polarization of Pc 4

To study the polarization of the shorter-period *Pc* 4, nine good *Pc* 4 with periods in the range 50–70 s were selected in each of the periods 04.30–08.30 (forenoon), 11.30–15.30 (midday) and 18.30–22.30 (evening). These were analysed by the FFT method and the polarization characteristics calculated. The results are given in Table IX which shows in each case the angle of

TABLE VIII. DIURNAL VARIATION OF *Pc* 4

Period (s)	*Time* 3–6	6–9	9–12	12–15	15–18	18–21	21–24	*Total*
50, 60	4	23	51	61	54	40	11	244
70, 80	1	10	5	14	11	14	3	58
90–110	2	3	9	3	7	2		26
120–150		12	10	14	27	22	4	89
TOTAL	7	48	75	92	99	78	18	417

The figures in the table are the number of occurrences of *Pc* 4 of period given in the first column, in the time interval given at the head of each column.

TABLE IX. POLARIZATION OF *Pc* 4

Forenoon Date	φ	*e*	*Midday* Date	φ	*e*	*Evening* Date	φ	*e*
15 Apr 1974	−29	−0.50 C	29 May 1974	−32	0.10 C	14 Apr 1974	3	0.76
23 Jun 1974	32	−0.56 C	22 Sep 1974	−44	−0.20 C	8 May 1974	−21	−0.14 C
19 Apr 1975	−51	−0.33 C	9 Oct 1974	60	−0.18 C	7 Sep 1974	−45	−0.06 C
29 Jul 1975	−9	0.60	23 Oct 1974	84	−0.64 C	6 Feb 1975	−44	0.23
30 Sep 1975	22	0.46	14 Dec 1974	−35	0.31	27 Apr 1975	45	0.89
4 Jun 1976	−50	−0.10 C	17 Mar 1975	−7	−0.42 C	28 Jul 1975	−52	−0.20 C
26 Jun 1976	−35	0.10	8 Nov 1975	−87	0.48	14 Mar 1976	−27	0.48
28 Jun 1976	−27	0.07	9 Apr 1976	54	0.67	12 May 1976	−38	0.21
18 Aug 1976	−45	0.02	2 Aug 1976	16	0.29	19 Jun 1976	48	0.00

φ Angle of polarization (in degrees). *e* Ellipticity. C Clockwise rotation.

polarization (φ, azimuth measured clockwise from geomagnetic north) and the ellipticity, the ratio of the minor to the major axis of the magnetic vector traced out on the Earth's surface; C indicates clockwise rotation.

The relative error in the digitizing of the time coordinate on the NE and NW traces is about 0.05 mm, corresponding to about 6 s or about 35° in the relative phase of the two components. This is not sufficiently large to account for the apparent random values of φ and *e*, and it appears from this rather small sample that there is no regular diurnal variation of the polarization of short-period *Pc* 4. Again, this will be investigated using the digital data.

Selection of Pc 5

The selection of *Pc* 5 is more subjective than in the case of pulsations of shorter period; long-period variations are fairly common, particularly in the evening, and it is difficult to decide when they are sufficiently constant in period, and continue for sufficient time to justify their classification as *Pc* 5. Fig. 12 is a half-hour section of a continuous pulsation with large amplitude and a constant period of 265 s for six cycles. This is a good example of a *Pc* 5; in other examples, the period is somewhat more variable and may change if the pulsation continues for more than an hour or so. In general, a duration of half an hour and a variation of period of not more than 20% of the mean period have been accepted for inclusion but a certain amount of subjective judgement has been exercised. In many cases, *Pc* 5 are seen most clearly on the *Z* trace due to increased induction effect at the longer periods, the induced shorter-period variations in *Z* being relatively small. In the case of the *Pc* 5 illustrated in Fig. 12, in which the horizontal component is polarized almost in the NW direction, the ellipticity in the NW–*Z* plane is 0.33.

Relation between Pc 5 and magnetic activity

The relation between *Pc* 5 and magnetic activity has been studied in the same way as in the

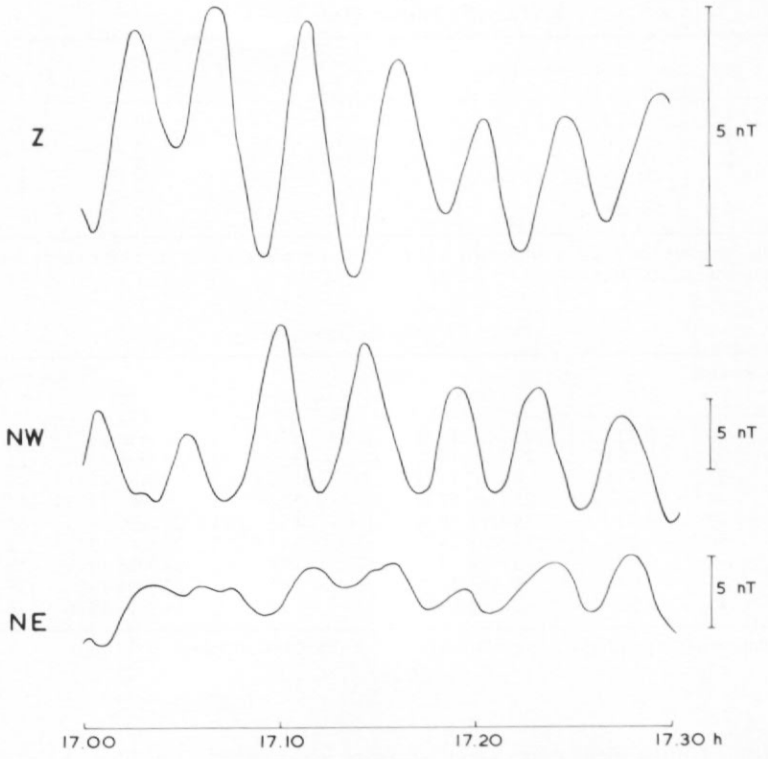

Fig. 12. *Pc* 5 on 11 April 1974; period 265 s.

case of *Pc* 4, and the results are also shown in Table VII. Again, there is no clear relation between the occurrence of *Pc* 5 and magnetic activity.

Diurnal variation of Pc 5

Table X gives the number of occurrences of *Pc* 5 arranged in three period groups, for each 3 h interval of the day. Clearly, *Pc* 5 is very markedly an afternoon phenomenon with maximum occurrence in the interval 18–21 UT.

TABLE X. DIURNAL VARIATION OF *Pc* 5

UT	*Period range* (s) 160–250	260–400	> 400	*Total*
00–03		2		2
03–06	1			1
06–09	9			9
09–12	9			9
12–15	3			3
15–18	20	9	1	30
18–21	53	12	2	67
21–24	19	7		26
TOTAL	114	30	3	147

The figures in the table are the number of occurrences of *Pc* 5 in the period range at the head to the column in the 3 h interval given in the first column.

Giant pulsations

Our representative example, Fig. 5, shows a packet of almost monochromatic waves with a range of about 6 nT and lasting about 30 min. Events like this are rare but very conspicuous and are identified as giant pulsations.

The FFT estimates in Table XI show the sharpness of the maximum in the power spectrum with a period of 56 s; a harmonic with a period near 29 s is also clearly visible.

A list of *Pg* events is given in Table XII, which includes a very powerful *Pg* that occurred in 1973. They all occur in the morning, mainly in the period 04–08 h local geomagnetic time; the pulsations are almost monochromatic with periods in the lower part of the *Pc* 4 range. The dominant sense of rotation was clockwise and the polarization was almost normal to the geomagnetic meridian.

TABLE XI. POWER SPECTRUM OF *Pg* OF 12 JUNE 1975

Period (s)	*Power* ((nT)² Hz⁻¹)			*Coherence*	
	D	*H*	*Z*	*D* : *H*	*Z* : *H*
143.1	5	13	0	0.77	0.54
117.4	5	5	0	0.09	0.52
99.5	9	1	0	0.18	0.49
86.3	3	5	0	0.65	0.65
76.2	4	4	0	0.82	0.40
68.3	3	5	0	0.29	0.76
61.8	6	85	3	0.66	0.45
56.5	347	2 074	48	0.99	0.99
52.0	18	83	3	0.79	0.89
48.1	4	4	0	0.26	0.78
44.8	1	1	0	0.92	0.72
41.9	2	3	0	0.79	0.73
39.4	2	5	0	0.69	0.54
37.1	2	3	0	0.86	0.73
35.2	3	1	0	0.63	0.31
33.4	7	1	0	0.76	0.70
31.7	1	0	0	0.79	0.84
30.3	0	1	0	0.81	0.38
28.9	6	7	0	0.90	0.96
27.7	3	3	0	0.90	0.73
26.6	3	2	0	0.93	0.72
25.5	1	3	0	0.90	0.88
24.6	2	2	0	0.85	0.97

TABLE XII. LIST OF *Pg*

Date	UT	*dd*	*t*	*Range* (nT)			φ	*e*
				H	*D*	*Z*		
11 Apr 1973	12	34	90	10	18		−82	0.56 A
23 Mar 1975	09	25	79	9	17	4	−80	0.37 C
12 Jun 1975	05	22	57	2.5	6	1	−85	0.42 C
29 Jul 1975	09	16	56	1	5	0.5	76	0.18 C
6 Sep 1975	05	30	70	2	3	0.5	−75	0.57 C
29 Oct 1975	06	60	67	1.5	5	1.5	77	0.01 L
22 Oct 1976	02	60	60	3	4	0.5	−86	0.65 C
22 Oct 1976	09	40	100	1.5	4	0.5	−82	0.40 C

dd Duration (in min).
t Period (in s).
φ Direction of major axis of polarization ellipse.
e Ratio of minor to major axis of ellipse.
C Clockwise rotation.
A Anti-clockwise rotation.
L Linear polarization.

IRREGULAR PULSATIONS, *Pi*

Selection of Pi

The fact that *Pi* are by definition irregular makes it difficult to identify them objectively. There are, however, a great number of events which can be identified as *Pi* without much doubt and a total of 1 472 has been listed (the full list), not counting those classified as rather poor or poor. Of these, 578 have been classified as better than fair (the shorter list).

The upper limit for the period of *Pi* 2 is defined as 150 s but a number of events with longer periods has been identified, mainly in the evening, with the characteristics of a *Pi* rather than that of a *Pc* 5; such events with periods up to 240 s have been accepted as *Pi*.

Relation between period of Pi and magnetic activity

During the analysis of the charts, it was clear that most *Pi*'s occur at night and that the period depended on the time of occurrence and on the magnetic activity. To study the variation with magnetic activity, the 12 h interval 19.30–07.30 was divided into eight 90 min intervals and the period of the *Pi* in each interval was correlated with a magnetic activity index. Initially, a detailed study was made for the two intervals 22.30–23.59 and 03.00–04.29 of the *Pi* in the full list. Regression equations were derived for each season between the period and the magnetic activity, both K_p, the planetary index of magnetic activity at the time of onset of the *Pi*, and $\Sigma K = 3\bar{K}$, the sum of the three values of K_p in the period 18–03 UT, were used. The values of the correlation coefficient (r) and of the coefficients t_o and k in the regression equation $t = t_o - kK$, where t is the period of the *Pi* (in seconds) and $K = \bar{K}$ or K_p, are given in Table XIII. The correlation coefficients, all greater than or very close to –0.5, show that there is marked correlation between the period and the magnetic activity, and for 03.00–04.30 a better correlation with $\bar{K}$ than with K_p. Moreover, while the constants for the summer are a little smaller than those for the other seasons, the differences are scarcely significant. Accordingly, no further attempt was made to derive the constants for each season. Table XIV gives the values of the constants for each of the 90 min intervals using the available data. Fig. 13 shows the period of the *Pi* for each time interval and each value of $\bar{K}$, and also the regression equations. The standard deviation of the measured periods of the *Pi* from the mean values in the four 90 min intervals 22.30 to 04.30 was 20 s.

TABLE XIII. RELATION BETWEEN PERIOD (t) OF *Pi* AND MAGNETIC ACTIVITY (K)

	$\bar{K}$			K_p			n
	$-r$	t_o	k	$-r$	t_o	k	
22.30–24.00							
Summer	0.50	123	10	0.56	124	11	38
Equinox	0.54	135	13	0.54	133	12	71
Winter	0.54	137	13	0.49	131	11	83
03.00–04.30							
Summer	0.71	117	16	0.50	110	12	54
Equinox	0.81	132	22	0.48	116	15	58
Winter	0.69	122	18	0.55	115	15	92

$t = t_o - kK$ (see text); correlation coefficient = r.

TABLE XIV. VALUES OF THE PARAMETERS IN THE REGRESSION EQUATION $t = t_o - kK$ S

	19½–21	21–22½	22½–24	0–1½	1½–3	3–4½	4½–6	6–7½ UT
$-r$	0.54	0.49	0.54	0.69	0.69	0.69	0.69	0.65
t_o	229	164	133	140	135	115	119	119
k	27	15	12	19	19	17	19	20

r Correlation coefficient.
The constants are discussed above.

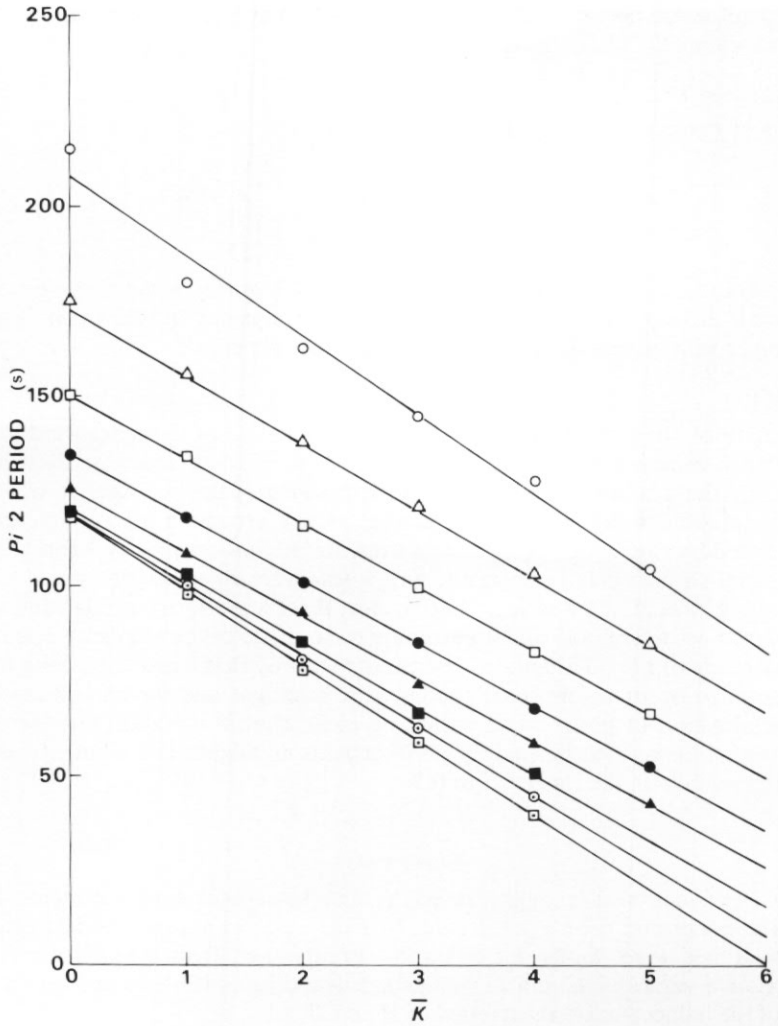

Fig. 13. Dependence of *Pi* 2 period on the index of magnetic activity, $\overline{K}$, defined in the text, for different UT intervals. The correlation coefficient, r, exceeds 0.99 in every case.

Diurnal variation in the frequency of Pi 2

Of the 577 *Pi* 2 in the shorter list, only 21 occurred between 07.30 and 19.30. The numbers which occurred in each of the 90 min periods were as follows:

	Number		*Number*
Before 19.30	8	01.30–03.00	112
19.30–21.00	28	03.00–04.30	94
21.00–22.30	49	04.30–06.00	78
22.30–24.00	65	06.00–07.30	33
00.00–01.30	97	After 07.30	13

It can be seen that these values are not symmetrical about local geomagnetic midnight, *Pi* 2 occurring somewhat more frequently later than earlier. Shorter-period *Pi* are easier to identify

and, as the typical period decreases during the night, this may account for the skew distribution of the diurnal variation.

Seasonal variation of Pi 2

The numbers of *Pi* occurring in each season are as follows:

	Full list	*Shorter list*
Summer	338 (395)	121 (141)
Equinox	466	201
Winter	668	255

The number in brackets is the corrected number for the summer when allowance is made for the lack of record early in 1974. It will be seen that the frequency in the winter is nearly twice that in the summer with intermediate values in the equinoctial periods.

Polarization of Pi

The polarization of about 60 *Pi* have been studied; about half of these occurred in the second half of 1976 when measurements of the components were being made at $2\frac{1}{2}$ s intervals on magnetic tape and the whole analysis, including the drawing of the hodograms, was carried out by a computer. In addition, about an equal number, in two groups in the autumn and spring of 1975, was analysed by digitizing the trace and drawing the hodograms by hand. As the pulsations are irregular, so are their hodograms, and a few were rejected, but most, often after a confused beginning, would show at least two cycles; these were fairly similar and enabled the sense of rotation to be determined and an estimate to be made of the ellipticity and of the direction of the major axis of the polarization. The results showed that there is a strong tendency for clockwise rotation to occur before local geomagnetic midnight and for anti-clockwise rotation thereafter. The direction of polarization shows no clear diurnal variation but there is a slight tendency for the major axis to be mainly E–W around midnight. The ellipticity showed little variation, being generally in the range 0.3 to 0.5.

Induction

The vertical field contains a field caused by the horizontal Earth currents induced by variations of the horizontal geomagnetic field. If there were no natural vertical field, i.e. if the measured vertical field were wholly due to Earth currents, then, from a number of observations in which the relative values of H and D changed, it would be possible to deduce the magnitude and direction of the induced currents in terms of H and D.

The induced vertical field, therefore, is correlated with H and D but the three components of the true field are unlikely to be correlated. So, by considering a large number of events and correlating the measured vertical and horizontal fields by computer methods, it is possible to deduce the parameters of the induced field.

This process has been carried out for 12 events, for which the power spectrum has been derived. The computer output lists the values of the parameters in the equation:

$$Z = (A_r + iA_i)\,H + (B_r + iB_i)\,D.$$

Other parameters which are computed are:

$$G_r = (A_r^2 + B_r^2)^{\frac{1}{2}},$$
$$G_i = (A_i^2 + B_i^2)^{\frac{1}{2}},$$
$$\theta_r = \tan^{-1} B_r/A_r,$$
$$\theta_i = \tan^{-1} B_i/A_i.$$

Table XV gives the values of these parameters with their standard deviations, the number (n)

TABLE XV. INDUCTION PARAMETERS

t	G_r	S.D.	G_i	S.D.	θ_r	S.D.	θ_i	S.D.	n	c
205	0.22	0.04	0.06	0.04	−20	9	30	33	10	0.89
125	0.24	0.06	0.08	0.06	−10	15	−4	42	12	0.69
90	0.19	0.05	0.09	0.07	2	20	−65	33	9	0.80
70	0.16	0.05	0.11	0.06	−5	37	−19	52	7	0.92
57	0.23	0.05	0.09	0.06	27	17	48	38	10	0.83
49	0.17	0.05	0.08	0.06	22	23	−58	40	10	0.75
42	0.17	0.06	0.07	0.07	27	23	−116	43	11	0.59
37	0.15	0.06	0.07	0.07	23	29	−138	64	10	0.56
30	0.12	0.05	0.06	0.05	−5	28	−166	58	9	0.65

For parameters G_r, G_i, θ_r and θ_i see text.
t Period (in s).
n Number of data segments.
c Coherence.
S.D. Standard deviation of the parameters.

data segments used in the regression analysis and the squared coherence (c) between the measured and predicted value of Z.

The number of data used is admittedly small but the coherence values are quite high, and the values of the parameters and their trend is clear. G_r is greater than G_i by a factor of 2 to 3 and increases from a value around 0.12 for pulsations of period around 30 s to a value about 0.22 for pulsations of period around 200 s, while the direction changes from about 20° for the shorter periods to about −15° for the longer period. Clearly, induction effects are small.

ACKNOWLEDGEMENTS

I wish to acknowledge the work of many British Antarctic Survey contract staff, who carried out the field measurements, and to thank Dr W. F. Stuart and the staff of the Geomagnetism Unit of the Institute of Geological Sciences, Edinburgh, for their help and advice.

MS received December 1977; accepted in revised form December 1980

REFERENCES

FINLAYSON, D. M. 1967. Characteristics of geomagnetic continuous pulsations at Halley Bay in 1963. *British Antarctic Survey Bulletin*, No. 11, 73–82.

KAISER, T. R., ORR, D. *and* A. J. SMITH. 1977. Very low frequency electromagnetic phenomena: 'whistlers' and micropulsations. (*In* FUCHS, V. E. *and* R. M. LAWS, *organizers*. A discussion on scientific research in Antarctica. *Philosophical Transactions of the Royal Society*, Ser. B, **279,** 225–38.)

LERWOOD, V. E., MACINTOSH, S. M. *and* W. F. STUART. 1973. The geomagnetic time dependence of pi2's and bays. *Journal of Atmospheric and Terrestrial Physics*, **35,** 1407–13.

STUART, W. F. 1972. Association between pi2 and bays at Lerwick and Halley Bay. *Journal of Atmospheric and Terrestrial Physics*, **34,** 817–27.

————. 1975*a*. Magnetosphere deformation at dpi initiation derived from conjugate observations. *Journal of Atmospheric and Terrestrial Physics*, **37,** 143–51.

————. 1975*b*. Conjugate polarization characteristics of pi2's. *Geophysical Journal of the Royal Astronomical Society*, **41,** 433–40.

————. 1976. Features of the generation of dpi's derived from conjugate observations. *Journal of Atmospheric and Terrestrial Physics*, **38,** 271–78.

————. *and* S. M. MACINTOSH. 1970. The polarization of micropulsations at Lerwick and Halley Bay. *Journal of Atmospheric and Terrestrial Physics*, **32,** 1007–13.

USHER, M. J., STUART, W. F. *and* S. H. HALL. 1964. A self-oscillating rubidium vapour magnetometer for geomagnetic measurements. *Journal of Scientific Instruments*, **41,** 544–47.

WESTWOOD, J. V. B. 1967. Geomagnetic micropulsations recorded at Halley Bay, 1963–64. *British Antarctic Survey Bulletin*, No. 12, 73–83.